Final Report: MOST 107-2813-C-008-053-M

Detector Traveling from Now to the Future: Study of the Calorimeter Performance for Future Colliders with the High Granularity Calorimeter in CMS and the Full Simulation based on FCC

Chih-Hsiang Yeh
Department of Physics and Center for High Energy and High Field Physics, National Central University, Chung-Li, Taiwan

Abstract

The discovery of Higgs boson at Large Hadron Collider(LHC) in 2012 opened a new door for particle physics. Since then, people have been hard-working on upgrading the LHC to the higher luminosity and center-of-mass (C.M.) energy, so to study the properties of Higgs boson and to discover new particles predicted by the physics Beyond Standard Model(BSM). Some people even proposed the idea to build new colliders, such as Future Circular Collider(FCC), etc. near the working LHC space now. For my study, I focus on three topics which are related to the detector performance. First, because the radiation tolerance problem and increasing pileup at High-Luminosity LHC(HL-LHC), the Compact Muon Solenoid(CMS) experiment at LHC will replace the current endcap calorimeter with a silicon-pad High Granularity Calorimeter(HGCAL). I did some studies on the performance for them using data from test beam in CMS and the Hexaboard of its electronics in National Taiwan University(NTU). Second, I used the GEANT4 full simulation to simulate the FCC detector under the very high energy condition and study the jet performance. We expect to help the future facilities to design a high resolution detector, and could have a large potential to find the new physics with the new detector.

Contents

1 Introduction

1.1 Motivation and Expectation

After identifying the Higgs boson at LHC in 2012, people are eager to explore the new particle and the physics BSM , such as dark matter candidates, Z' bosons, heavy Higgs, and so on. CMS and ATLAS collaboration are also upgrading the detectors to improve the functions to cope with the new challenging conditions in the future colliders. For the operation in the future, one of the most important issues of detector performance is: How can we boost the efficiency of the distinguishability of signal from the background?

In the upcoming HL-LHC era, the pileup will be raised significantly compared with the condition the LHC is operating at currently. Therefore, first of all, we need to identify the particle very well. Otherwise, we are not able to reject the unwanted contaminant particles. My first topic with HGCAL in CMS focuses on the particle identification with electrons and pions. Because we will keep searching on more new physics with the electron final states , but some pions will be misidentified as the electrons, our requirements are removing these mistagged "fake" electrons. It is expected that we can find out the optimized cuts for them and apply in the cut-based analysis, aiding the signal and background studies that are very sensitive to pions. Furthermore, I studied some cross-talk phenomena on the PCB boards which are attached with the sensor used in the HGCAL, and try to find out the correlation between the injection pulse strength and cross-talk. We expect to understand the noise created in the electronics and reduce them in the future.

Some have proposed colliders with the higher C.M. energy for the next generation, such as Future Circular Collider (FCC), Circular Electron-Positron Collider (CEPC), Super proton-proton Collider (SppC) etc. When those colliders operate, other crucial problems with higher C.M. energy will arise. Under these circumstances, the jets from the segmentation will be very boosted. In this case, we need to explore other ways to look into this boosted jets structure. Otherwise, we can't separate the signal from the background very well. My second topic with FCC detector focuses on the boosted conditions, using different jet substructures with various configurations of the FCC detector to see whether the smallest detector configuration will give the best separation power to distinguish signal from the background.

1.2 Summary for research topics

The research activities of Chih-Hsiang Yeh from July 1, 2018 to Febraury 28, 2019 includes the following:

- Research with electronics of HGCAL : Cross-talk studies with the no sensor based Hexaboard in NTU
- Research with HGCAL in CMS : Pion-rejection studies with a CMS HGCAL test-beam prototype Electromagnetic calorimeter(ECAL)
- Research with simulation FCC detector : Studies of granularity of a hadronic calorimeter for tens-of-TeV jets at a 100 TeV pp collider

I will describe in more detail for all of the items above.

2 Cross-talk studies with the no sensor based Hexaboard in NTU

Cross-talk is the one basic phenomenon exist in the electronics, which is a signal transmitted on one circuit or channel of a transmission system creates an unwanted effect in another circuit or channel. For example, it has two types cross-talk could happen:

- Correlated cross-talk
  The capacitors in the circuit are too closed wth each other. One capacitor is charging, and it could influence the other capacitors by the EM effect.
- Anti-correlated cross-talk
  It could happen in the circuits which have the problem in power supplication. When the process in one channel doesn't have enough energy to process, it could "borrow" the energy from other channels, and lead to the cross-talk also.

Then, both of them will lead to giving out the wrong signal from the electronics. We need to quantify this value and know more about this kind of noise, otherwise, it will be a big problem when we use this electronics to reconstruct the events from the sensor.

I did this study with Prof.Stathes Paganis, Prof.Rong-Shayang Lu, master student Chia-Hong Chein from NTU, and Prof.Shin-Shan Eiko Yu from NCU. The contributions of Chih-Hsiang Yeh to this study includes the following:

- Study the correlation between the stability of pedestals(SCA0) and other SCA sampling.
- Study the correlation between the injection pulse strength and the cross-talk.

I will describe the detail as following.

2.1 Experiment apparatus and Event reconstruction

For the experiment, we used the electronics which are composed of three parts, including the module (version 2), RPI Hexa and Raspberry Pi 3(RPI). In the Figure1, it presents the electronics and data flow we applied. For the module, it also be called "Hexaboard", because of its shape is hexagonal-like. The main power of it is to collect analog signal and convert them into the digital format. It can be bonded to silicon sensor, such as the HGCAL, to collect real charge from particle go through the sensor and do physical analysis. It also can be given the electrical pulse manually to simulate the sensor-attached condition. For the RPI Hexa, it is the bridge between FPGAs and Raspberry Pi(RPI). When the signal come out from the four CHIPs of hexaboard, first of all, we will collect them to the "slave" FPGA on the HexaBoard. Then after finishing collecting the data, the "slave" FPGA will transfer the data to MAX10 FPGA("master" FPGA) on the RPI Hexa. For Raspberry Pi 3(RPI), acting like the small computer, can do many things communicate with the hexaboard. The main power for it is to receive

the MAX10 data and can encode to read back the data, and finish reconstructing the events.

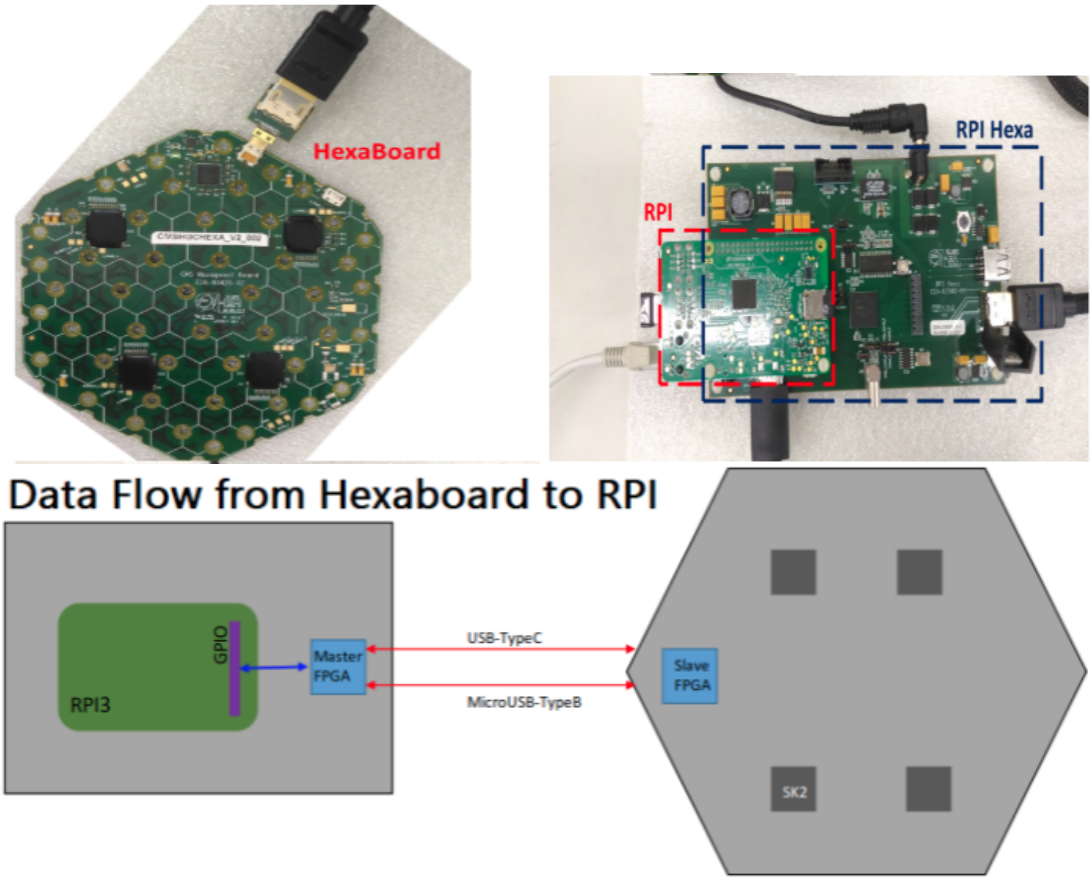

Figure 1: (Top left) The Hexaboard which was applied in the study. On the board, there are four SKIROC2cms CHIPs (black hexagonal) used to receive the electrical pulse which is given by the cable, and give out the signal to the Hexa RPI. (Top right) The Hexa RPI and RPI which is applied to transform the data and communicate with Hexaboard. (Down) The data flow pictures for introducing the data transfom from Hexaboard to Hexa RPI and RPI.

Every SKIROC2cms CHIP on the HexaBoard corresponds to 64 channels, while each channel has its own readout circuit(Pre-amplifier, shapers,etc.). In each event(run), it recorded 30 numbers to reconstruct the event for every channel. Totally 30 numbers are given by 13 ADC counts in both highgain(HG) and lowgain(LG) plus 2 TOTgain(Time Over Threshold) and 2 TOAs(Time Of Arrival). The 13 ADC counts of HG and LG come from 13 SCA(Switched Capacitor Array) units in the circuit, which sample the input signal every 25ns[1]. They can be used to define the hardware noise and differences between each capacitor. At the same time, we recorded the time stamp with the pulse trigger[2] for each event. Time stamp label the whole pulse in order, so we can use

[1]There exist thirteen different capacitors with the number SCA0, SCA1....SCA12, and they will record one ADC value in order every 25ns for the each channel of CHIPs. When going to SCA12 and finishing recording, it will return to SCA0. The order of SCA numbers are not related to the order of the electrical pulse we give, but the time stamps are.

[2]In real case, it recorded the starting SCA and the end of SCA with roll position array when the pulse

the time stamp to mark the pulse location, specially for the peak of pulse.

2.2 Events and Methods for analysis

For simplifying the study, we used the Hexaboard without the sensor on it. In this studies, we used two types of runs to do the researches through the whole process:

- Pedestal run: Run without injecting the electrical pulse, and record the non-pulse run to be our reference.
- Charged run: Run with injecting the electrical pulse to the certain channel, and record the with-pulse run to do the study.

Be attention with, because we simulated the sensor-attached condition, and sensor only apply the 32 channels on the Hexaboard in real life, we used 32 channels of the Hexaboard to study. In the Fig.2 is the channel map that we used in the study.

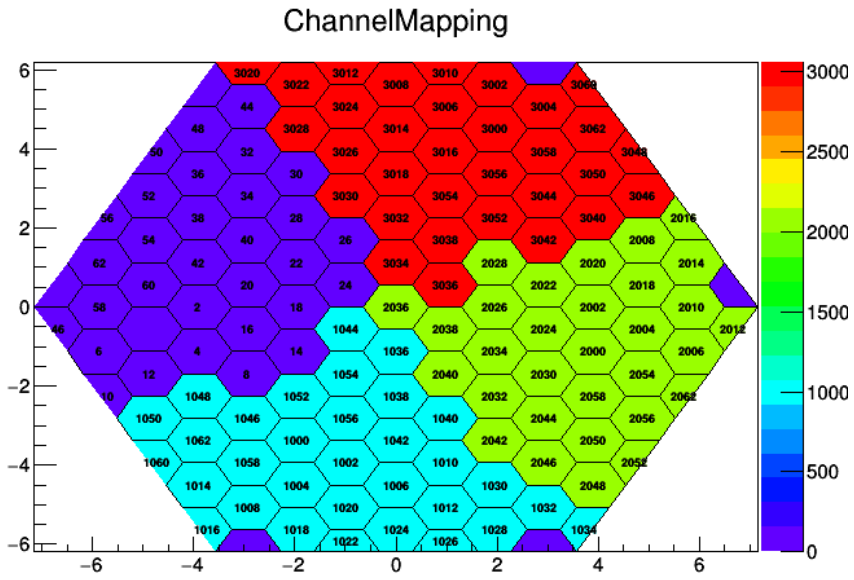

Figure 2: The channel map which was applied in the research, there are four regions with the different color represent the different SKIROC2cms CHIPs. A digit in thousands is the order of the CHIPs, and a digit in tens and ones represent the channels on each CHIPs.

The following three cases which were used in our studies are shown in the fig.3. (1)Pedestal run were used to evaluate the pedestals and noise for each channel. The value of mean of ADC-counts will be defined as the pedestal value from each channel, and it is the hardware-dependent(SCA-dependent) value. (2)Charged run were used

trigger is on and off, and rearrange the SCAs with this array as the time stamp, so it can be specified as the pulse information.

to record the responses with ADC-counts values from every channel with the electrical pulse injecting, and simulated the real physics. (3)In the end, the "Pedestal-subtracted" value will be used in our study for subtracting the "reference". The mean value of the ADC-counts for it is calculated after Charged run ADC-counts subtract the mean of ADC-counts from Pedestal run with same SCA number. And the error(width of gaussian) means the noise in the channels including the electronics noise, sensor noise(if it is installed), etc. Note, in the study, we always used SCAs of HG to do. For simplifying the case, we fixed the injected-channel to number 20 in CHIP 0 and saw all cases.

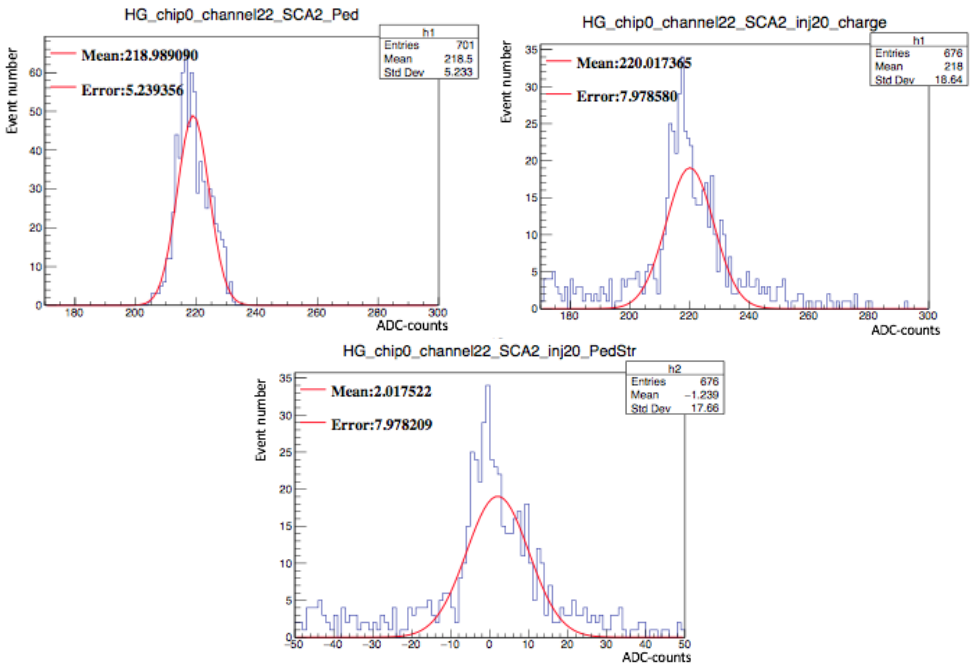

Figure 3: These figures perform the histograms that using in the study. All this cases are shown with fixing at SCA=2 and channel=22. (Top left) The pedestal run histograms which is used to calculate the pedestal and noise. Fitting the line is to get the mean of ADC-counts. (Top right) The charged run for example. (Down) The pedestal-subtracted case is shown. Also fit the line to get the mean and error of ADC-counts, and use in the study directly

2.3 Results and Conclusion

First of all, because the first SCA (the 0th) is useful for making on-line pedestal subtraction (because there may be some low frequency noise), and usually our signal comes after SCA0, we need to explore the correlation between the stability of pedestals(SCA0) and other SCA sampling. In the Fig.4, we can see that the nearest channel of the injection channel (channel 20) with channel 18 and 22 as examples, the stability of them are very good. Because the fitting lines are pretty flat in both of them, and that means in the different SCA number other than SCA0, they are slightly different. And we can see the same condition in other channels also.

Second, we wanted to explore the correlation between injection pulse strength and the cross-talk. In real physics, because particles will have different energy individually in the collider, they will see the different pulse strength in the real case. At there, we

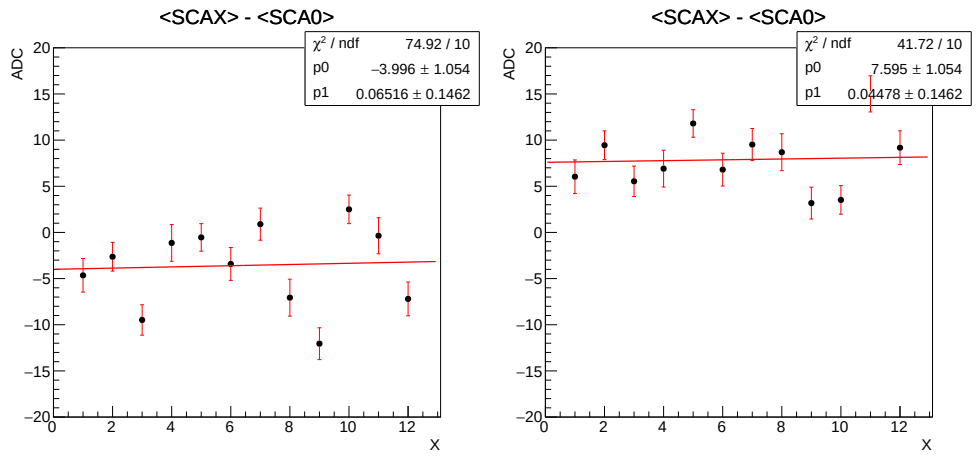

Figure 4: The figures show the difference mean of ADC-counts between the first SCA and other SCAs. (Left) The channel 18 response and (Right) The channel 22 response.

wanted to see whether the different pulse strength will give out more or less the cross-talk. In the fig.5, they show that the mean and error values from Pedestal-subtracted value for different DAC of injection pulse. The results for them are quiet obviously showing that the cross-talk in two cases:

- Anti-correlated cross-talk
  DAC from 0 to 1000: No matter the closer or farther the channels, the slopes are negative for all of them. That means the channels, except the injection channels, are borrowed the energy by injection channels.
- Correlated cross-talk
  DAC after 1000: When the channels are closed to the injection channels, the slopes are bigger compared with the channels which are farther from the injection channels. That means, the injection channels give more energy to the closed channels compared with the farther channels.

For the conclusion, we can see from our study that the cross-talk exist in the Hexaboard, and we used the ADC-counts from the Pedestal-subtracted values to quantify the cross-talk. We expected that this study can help to quantify the cross-talk and can decrease it in the future.

3 Pion-rejection studies with a CMS HGCAL test-beam prototype ECAL

In most cases, the electrons leave most of the energy in ECAL by the processes of pair production and bremsstrahlung. Different from them, Chagred-pions deposit most of the energy in Hadronic Calorimeter(HCAL) through the process of segmentation. Unfortunately, in some cases, those pions could give out the fully Electromagnetic(EM) showering in ECAL, and put most of the energy in it. If we can't explore the way to tag those pions and reject them, it will be very terrible. Because they will be misidentified as the electrons, and those "fake electrons" could contaminate with the real electrons. In addition, it could influence the analysis which is sensitive to the electron/pion dis-

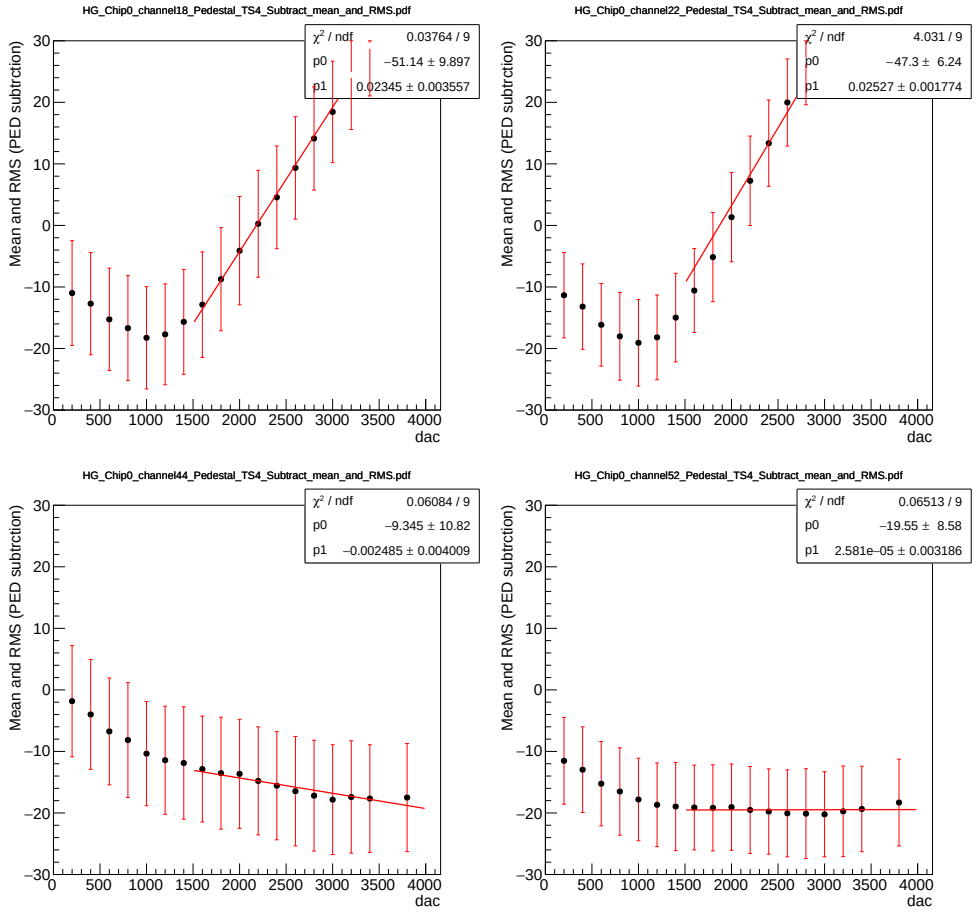

Figure 5: These figures present the preliminary results for the correlation between the different DAQ input and Pedestal-subtracted mean and error. The Top left and right pictures perform the channel of 18 and 22, which are closed to the injection channel. The down left and right pictures show channel of 44 and 52, which are farther from the injection channel.

tinguishability. We expected to solve this issue and help the physics analysis with this type of background in the future.

Because of the significant challenges for radiation tolerance and event pileup on the detectors of the CMS experiment at LHC, they will replace the current Endcap calorimeter with a Si-pad HGCAL, a new generation state-of-the-art calorimeter, which can perform 3D imaging of the shower as well as provide 30ps timing. To test the performance of HGCAL, including calibration, particle identification, etc. before it will be installed in CMS Phase II upgrade , we did the "test-beam"(Fig.6), which was held to incident the test particles, such as electron, pion and muon into HGCAL prototype, and analyze its performance from the information of the hits come out with the detector. At the same time, The Monto Carlo(MC) samples are provided with the same prototype of the detectors to let the people study as well. We used the test-beam MC samples which are done in CMS on June and October 2019 to do this study. The group of test-beam divided the studies into many different topics, and my topic was in the section of "electron/pion identification".

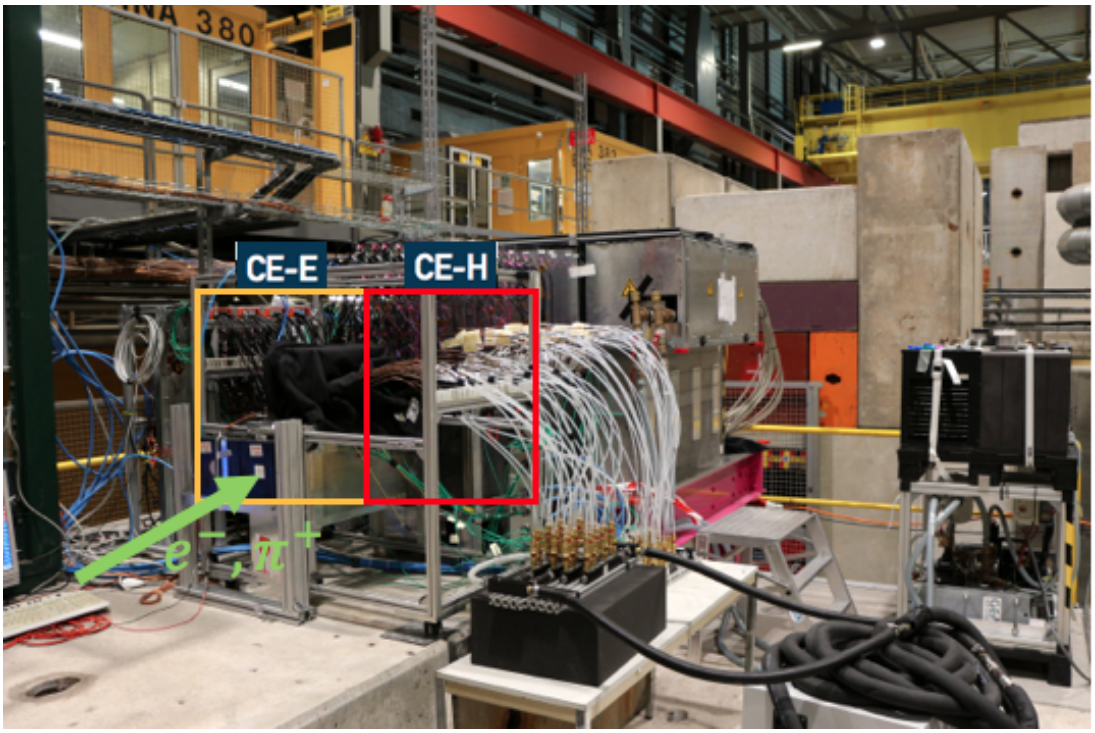

Figure 6: The figure show the test beam experiment setup in October. The orange and red lines box mark the CE-E and CE-H part of the detector including the module(in the metal box) and readout electronics.

Charged-pion tagging and rejection are one of the strong points of HGCAL. Traditionally the most powerful discriminants for pion rejection are lateral shower containment and longitudinal energy leakage in the back of the EM section of HGCAL. In this study we explore the capability of HGCAL to tag pions that are fully EM-showering in the ECAL and they pass the transverse containment and leakage from the back requirements. For our expectation, we wanted to find the best cuts and invited the new variables to distinguish "fake electrons" from "real electrons".

I did this study with Prof. Stathes Paganis, Prof. Rong-Shayang Lu, master student Chia-Hong Chein from NTU, Dr. Shilpi Jain from University of Minnesota and Prof. Shin-Shan Eiko Yu from NCU. The contributions of Chih-Hsiang Yeh to this study includes the following:

- Study the optimized cuts for finding the "fake electron" from pions, and introduce the new variable with the longitudinal segmentation using the test-beam MC from June.
- Apply the found optimized cuts and new variable in test-beam MC from October to see the electron efficiencies and pion rejections.

I will describe the detail as following.

3.1 Introduction for HGCAL

During the Run 1 (2010-2012) in LHC operated at $\sqrt{s} = 7\,\text{TeV}$, delivering $\approx 6\,\text{fb}^{-1}$, and at $\sqrt{s} = 8\,\text{TeV}$ in 2012, delivering $\approx 23\,\text{fb}^{-1}$. The most significant physics results

from this period was the discovery of the Higgs boson, and along with the Nobel prize for it in 2013. After Run 1, Run 2 started in 2015 at a C.M of $\sqrt{s} = 13\,\text{TeV}$ and the instantaneous luminosity, reaching to the value for $1.7 \times 10^{34} cm^{-2} s^{-1}$. In the Figure.7, it shows the summary plot for the luminosity from Run1 to Run2. Surprisingly, it operated the exceed value compare with the original design. More studies with this unbelievable operation, such as Higgs boson, SM processes, BSM, will be carried out.

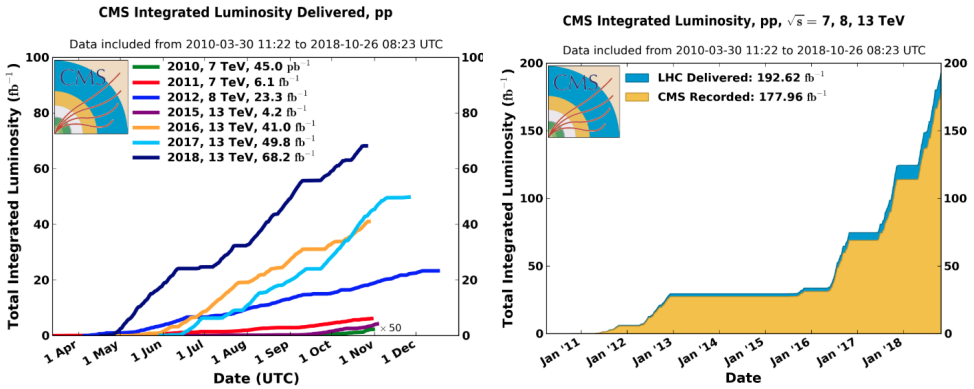

Figure 7: The figures show the summary plot of luminosity from the Run1(2010-2012) to Run2(2012 to 2018) in LHC. The left is the luminosity for the individual years, and the right is the totally integrated luminosity from 2010 to 2018.

For the future in Run3(2023), LHC intended to accumulate around $300\,\text{fb}^{-1}$. After the third long shutdown (LS3), they plan to design the value to the instantaneous luminosity at $5 \times 10^{34} cm^{-2} s^{-1}$ with the target of integrating around $3000\,\text{fb}^{-1}$ by the time of mid-2030s, and it will go into the HL-LHC era. The corresponding mean number of collisions (pileup) per bunch crossing will be 140. In addition, the LHC has the ability to deliver 50% higher values for both the instantaneous and integrated luminosities.

In this case, It will bring out the two significant issues in the HL-LHC era: (1)radiation damage and (2)event pileup on CMS detectors, especially for calorimetry in the forward region. As part of its HL-LHC upgrade program, the CMS Collaboration is proposing to build a HGCAL to replace the existing endcap calorimeters. There are many requirements for the HGCAL upgrade to let it preserve the good performance. Write some of them as following:

- This detector must be "radiation tolerance", otherwise, it will happen the unrecoverable condition, same as the circumstance of scintillator now in CMS. To solve this issue, active layer with the silicon sensor will be applied in the HGCAL.
- This detector need to be designed with the find granularity for lateral and longitudinal segmentation:
  - For the lateral part, it can help with separating two showers and can observe the narrow jets.
  - For the longitudinal part, it can help us to probe the longitudinal development of showers, providing good energy resolution, and also can know more about the patterns in the physics processes.

  Both of them can remove the "pileup event" if they are great enough to

distinguish processes of different particles.

The HGCAL prototype consists of an electromagnetic compartment (CE-E) followed by a hadronic compartment (CE-H) with Forward region(FH) and Backward region(BH) in the Fig.8. For the CE-E, it consists of 28 sampling layers with a depth of approximately 26 X_0 and 1.7 λ. In the Fig.9 top left shows one sampling layer of the CE-E. The element of active layer for it is a hexagonal silicon sensor, which is sandwiched between layer of WCu (75%, 25%) baseplate and a printed circuit board(PCB), which is used to study my cross-talk studies in NTU, that carries the front-end electronics to form a silicon module in the Fig.9 top right. Modules are tiled on a Cu cooling plate, which together with the two WCu baseplates form one absorber layer. The alternate absorber layer is formed by lead planes clad with stainless steel (SS) sheets that are placed on module-cooling plate sandwich.

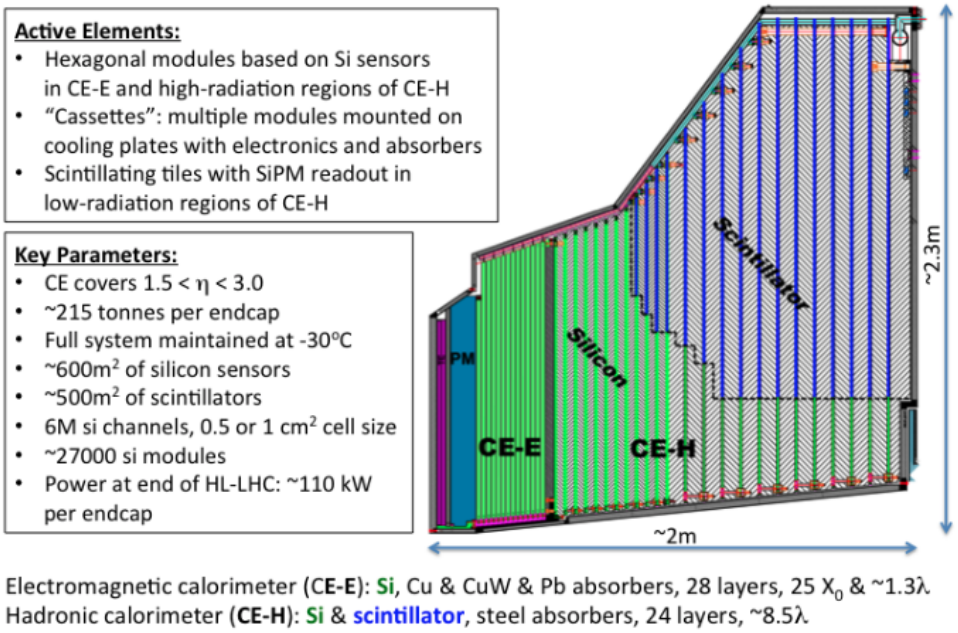

Figure 8: Summary for the basic design and coverage of the CMS high-granularity Endcap Calorimeter (CE) including CE-E and CE-H

For the hadronic compartment of HGCAL, they consist of 12 planes of thick SS plates followed by another 12 SS planes with different thickness. Between these absorber plates sit silicon modules(show one sampling layer in Fig.9 down left) in most regions and silicon modules mixed with scintillator tileboards(show one sampling layer in Fig.9 down left) in part of low-radiation regions mounted on a copper cooling plates to form the wide cassettes. These cassettes are similar to those in the EM compartment, but include sensors on only one side of the cooling plate, which are formed as a separate mechanical structure. This leads to a total interaction length with number 10.7λ, including the CE-E and the neutron moderator layer in front of the calorimeter. All layers are read out for use in energy measurement, but only alternate layers in CE-E, and all in CE-H, are used for producing L1 trigger primitives.

In the test-beam, we used the material based on prototype of HGCAL written below, but for the detail of its, each components will use the CMS phase 2 design. I will write

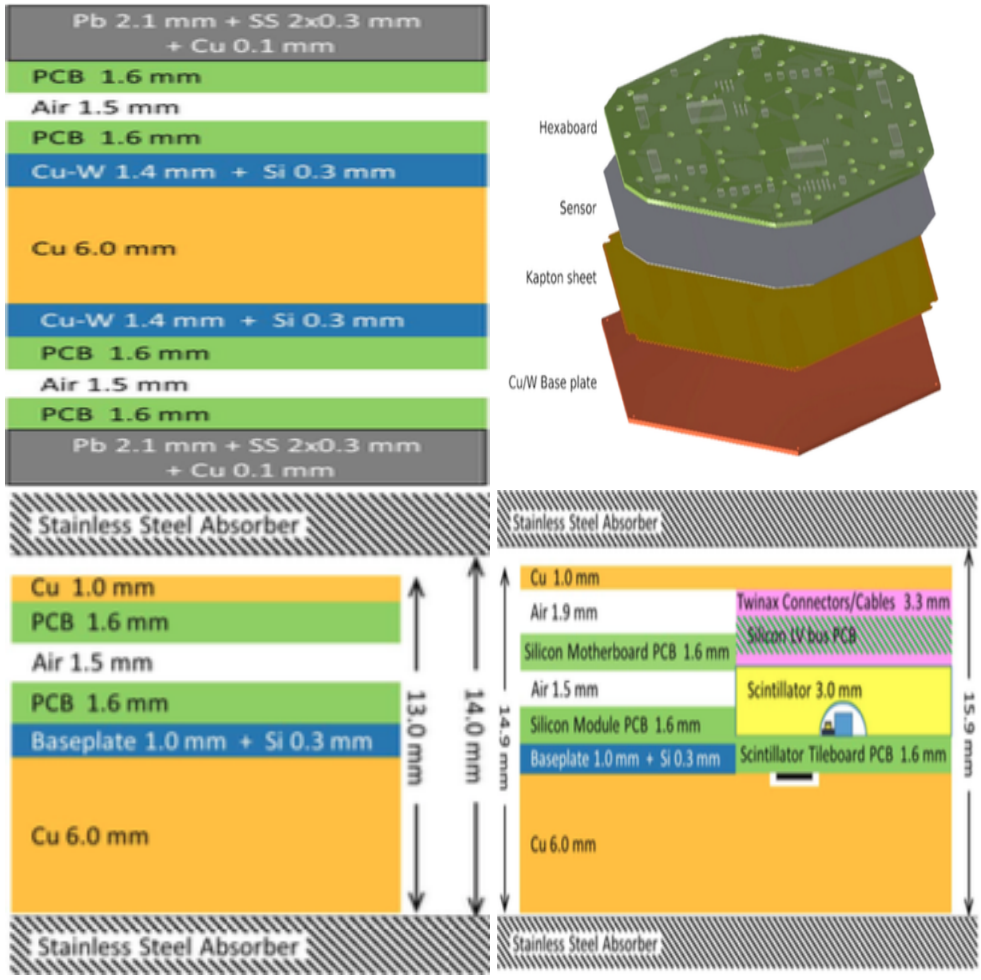

Figure 9: The figures show the different material arrangement in the different part of the detector. The top left is the one sampling layer of the CE-E. The top right show the silicon module used in the CE-E and CE-H. The down left is the one sampling layer of the CE-H which is sit on the high-radiation region. Oppositely, the down right is the one sampling layer of the CE-H which is based on the place with low-radiation.

the results of the test-beam in 2018 on June and October.

3.2 Tag-and-probe the optimized cuts and new variable with June test-beam MC

Because we wanted to tag the "electron-like"(e-like) pion, we need to explore the properties for the electron first, including shower shape, energy deposition, etc. in detector. And then, apply all of them in pion runs to tag those bad pion. I will describe the detail for the cuts and selections as following. In this studies, we used the sample with 50GeV electron and pion MC.

The first selection, because electron and pion have very different shower shape(width) on the transverse plane in ECAL, we studied on them at starting. From the theory, it tells us that electron has the narrower shower shape than pion in ECAL, we explored the cut with the different number of rings on the transverse plane of detector. In the

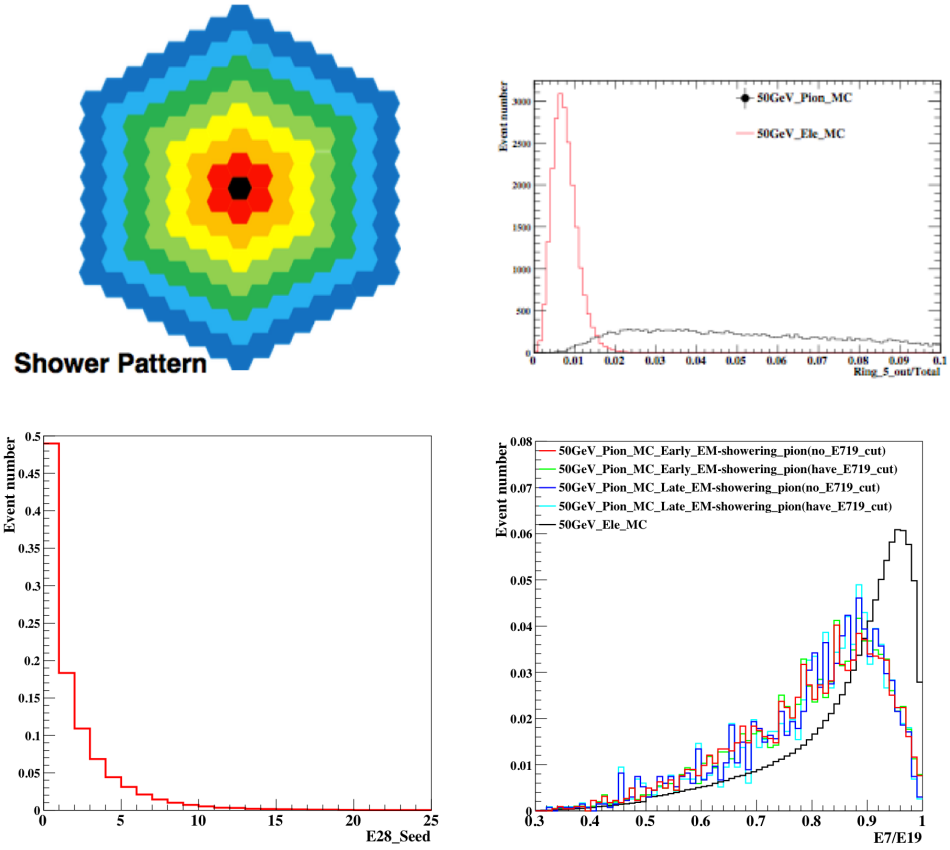

Figure 10: These figures present the cuts we used in the studies. Top left is the shower pattern on the transverse plane in the detector. Different rings mean the different sizes of the clustering on it. For example, the 5-Rings means the fifth circle calculated from the black pad to the shadow green. The top right plot is the energy distribution of $\frac{\text{energy out of the 5 Rings}}{\text{total energy}}$. The down left is the last layer energy with electrons. The down right is the cut with $\frac{\text{energy in 2 Rings}}{\text{energy in 3 Rings}}$, we plot every layer $\frac{\text{energy in 2 Rings}}{\text{energy in 3 Rings}}$ value with and without the $\frac{E_7}{E_{19}}$ cut

Fig.10 top left shows the distribution plot of ring. In the end, we chose the energy of 5 Rings for being the cuts. Fig.10 top right is presented to show the cut we used with "$\frac{\text{energy out of the 5 Rings}}{\text{total energy}}$". Because we can see in the plot, the energy of electrons showering are collected out of the 5 Rings with at most 1% compared with total energy in ECAL. We chose this standard to tag the e-like pions first. Although, it is the tight cut because it also discarded some of electrons as well, but we wanted to make sure that we cut-off the bad pion really. We called this cut as "5-Rings cut".

The second selection, because we wanted to select the "fully EM-showering", and we didn't have the information of HCAL energy in this month test-beam, we only could use the "poor man's solution"-finding the last layer energy of electrons and using it to be our cut. In the Fig.10 down left is the plot which was used to find the cut of last layer energy with the events which passed 5-Rings cut . Eventually, we used the last layer energy smaller than 20MIPs to tag the fully showering events, we called this cut

as "The last layer energy cut".

The third selection, it was the cut always used to find the EM-showering in pion traditionally, and related to the shower shape also, similar with the first selection. In every run, we applied the cut with "$\frac{\text{energy in two Rings}}{\text{energy in three Rings}} = \frac{E_7}{E_{19}}$" need to be at least 0.75 at the shower depth maximum layer. Shower depth(unit:X_0) is the energy weighted in the detector, it means the center-of-energy in the shower. In the Fig.10 down right shows the events with the values of $\frac{E_7}{E_{19}}$ of all layers. Compare between with and without the cut, most of the events with cut have bigger value than without the cut, this means we cut-off some of the boarder shower shape events in pion runs. Both of Early EM-showering and Late EM-showering in the plot are two kinds of e-like pion, will describe the detail later.

The fourth selection, because we applied those cuts from first to third, and we looked the shower depth for those passing events in the Fig.11, we found there exists two types of electron-like pion with the cut described in the next paragraph:

- Early EM-showering: The events have the similar shower depth with the electrons in ECAL, which means the energy distributions for these events are similar with the electrons. We can't distinguish them from electrons very well.
- Late EM-showering: The events have the late showering compared with the electrons in ECAL, and they put most of the energy in the backward ECAL, we can use some variables to distinguish this kind of pion from electrons.

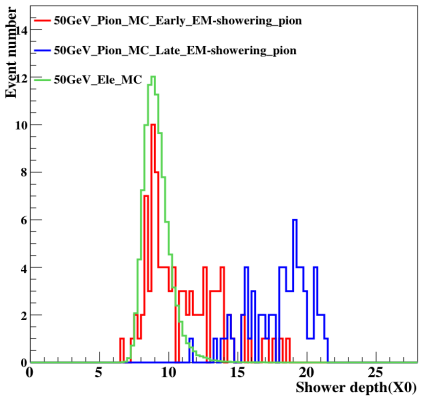

Figure 11: This figure shows the shower depth for both Early EM-showering and Late EM-showering.

We show some event display for normal electron and pion showering, Early EM-showering and Late EM-showering in Fig.12. And we present the event display in the We used the cut that, we require a consecutive number of hits in CE-E starting from the first layer and checking until the 14 Layer. We record the first layer found with more than 3MIPs. And at least 2 consecutive layers with more than two seeds with Energy>3MIPs. If the layer of start showering is from the first to fifth layer, we called it "Early EM-showering", on the other hand, if it starts at sixth to later layers, we called it "Late EM-showering". For note, because this is the convenient way to let us

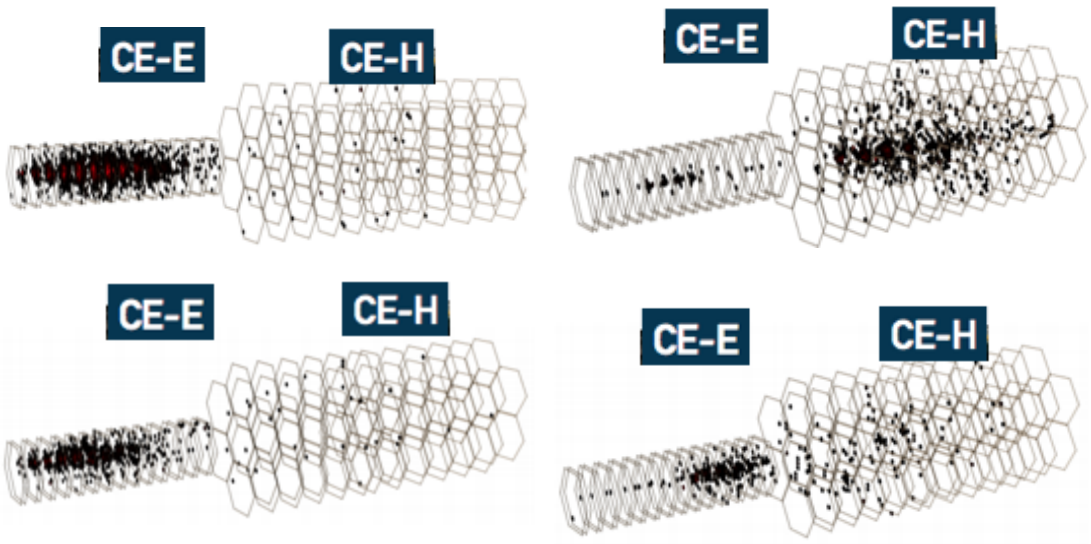

Figure 12: These figures show the event display with the cases which are the used to probe in the studies. (Top left) is the normal electron, most of the energy put in the CE-E, oppositely, (Top right) is the normal pion, which put most of the energy in CE-H. The both cases below the normal particles are the "e-like pion" cases, which we target to distinguish them from the normal electron. The left plot is the case for "Early EM-showering" and the right plot is the case for "Late EM-showering".

see the dynamic of the shower in ECAL approximately, we used this cut to distinguish them. In the real case, we don't do this cut, just used one variable to distinguish "both" of them from electrons. I will show the results later.

Tight cut types	value
5-Rings cut	> 0.99
The last layer energy	< 20MIPs
$\frac{E_7}{E_{19}}$	> 0.75

Table 1: E10/Etotal Tight cuts selection used in June test-beam

Until now, we can see the one strong point of the difference between electron and e-like pion - the shower energy deposit in the ECAL. Because some of them put energy in the different section of succeeding layers in ECAL, specially for comparing the electrons with Late EM-showering. In this case, we thought about the variables with "longitudinal segmentation" with ECAL. We developed the discrimination variable as following:

$$E_{10} = \frac{E_{\text{first 10 layers energy}}}{E_{\text{total energy}}} \tag{1}$$

Intuitively, because the electrons put most of the energy in the front of the detector, they will have the bigger value for E_{10}. Oppositely, for the e-like pions, because they put all of the energy in the different sections, they will have many values for E_{10} from all events. In the Fig.13, we can see that we can use E_{10} to reject some of e-like pions out of the electron region.

In my study, we need to find the critical point of E_{10} to be the threshold, because we wanted to reserve the electrons as many as possible, and cut-off the bad pions for

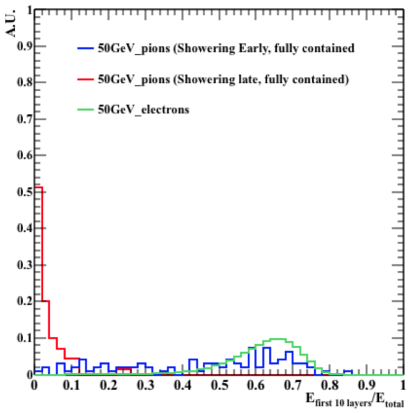

Figure 13: The E10 value for electrons, Early EM-showering and Late EM-showering.

our best. We used the quantities about the "Electron Efficiency" and "Background Rejection" as our standard in the following formula, to see whether this cut is good:

$$\text{Electron Efficiency} = \frac{\text{Pass electrons}}{\text{Total electrons}} \tag{2}$$

$$\text{Background Rejection} = \frac{\text{Total e}-\text{like pions}}{\text{Pass e}-\text{like pions}} \tag{3}$$

Our goal is to cut-off the most e-like pion with the highest background rejection (pass the least e-like pions) in (2), but reserve the most electrons with the highest electron efficiency. (pass the most electrons) in (3).

First, we tried to use the critical point at 0.2, 0.3 and 0.4, and see whether it can give us the best results. In the Table.2, it tells us that the background rejection is good (more than half of e-like pions are rejected), but we hoped that our electron efficiency will go to 99.8% or more. On the other hand, we still wanted to keep the electrons alive after the higher critical point to reserve most important researches on them.

E10/Etotal cut	Background Rejection	Electrons Efficiency
>0.2	2.15+/-0.18(stat)	99.85%+/-0.01%(stat)
>0.3	2.53+/-0.24(stat)	99.30%+/-0.01%(stat)
>0.4	2.74+/-0.28(stat)	97.32%+/-0.01%(stat)

Table 2: E10 cuts of Electrons Efficiency and Background Rejection comparison with point 0.2,0.3 and 0.4

In this case, we tried to use another points near 0.2 and see whether we can get the great results without losing more electrons. In the Table.3, it said that near the point 0.2, it can reserve most of the electrons near 99.9% and can get the background rejection with the expectation value near 2 (Half of rejection).

For the conclusion of this month test-beam results, we found that the Background Rejection can be near 2 without killing many electrons with 99.9% Electron Efficiency. For our expectation, we wanted to apply this cut in the October test-beam, to see whether we can see the similar results.

E10/Etotal cut	Background Rejection	Electrons Efficiency
>0.16	2.02+/-0.15(stat)	99.93%+/-0.01%(stat)
>0.18	2.07+/-0.16(stat)	99.89%+/-0.01%(stat)
>0.20	2.15+/-0.17(stat)	99.85%+/-0.01%(stat)

Table 3: E10 cuts of Electrons Efficiency and Background Rejection comparison with point 0.16,0.18 and 0.20

3.3 The results of application in October test-beam MC

In this month test-beam, because we had the information of HCAL, we used the cut no more than 0.4% energy fraction in the HCAL energy to replace the poor man's solution. And also, we changed some parameters of the cuts to get the best results. In the Table.4, the summary table for the cuts is shown.

Tight cut types	value
5-Rings cut	> 0.99
$\frac{\text{HCAL total energy}}{\text{ECAL total energy}}$	< 0.004
$\frac{E_7}{E_{19}}$	> 0.85

Table 4: Tight cuts selection used in October test-beam

In the June test-beam, we only did the rejection for E_{10} after the tight-cut selections. In this month, we wanted to studied the power of the cuts from tight-cut selections to E_{10}, it means we wanted to study totally how many e-like pions will be rejected after all cuts. We have two steps rejection, and we used the same definitions with the equation (2) and (3).

- Tight cuts rejection power:
  This is the first step rejection study. Because we need to find out the e-like pions with the cut in the Table.4 first, and then we can use our segmentation variable to reject them for the next step. For this step, we found that the number of the background rejection is 3600. Most of the pions are rejected by those cuts.
- E_{10} cuts rejection power:
  This is the second step rejection study. After we found out the e-like pions, we used the discrimination variable which we have invited in June test-beam,E_{10}, to distinguish them from the real electrons. In this step, we used the critical point at 0.18,0.20 and 0.22, to see whether at the critical point near 0.2 will give us the good results. In the Table.5 summarize the results for them. Although, this time didn't have the better results compared with the June test-beam, we still got the number about 1.5.

E10/Etotal cut	Electron Efficiency	Background Rejection
> 0.18	99.56%+/-0.01%(syst)+/-0.20%(stat)	1.52+/-0.27(stat)
> 0.20	99.05%+/-0.01%(syst)+/-0.20%(stat)	1.53+/-0.26(stat)
> 0.22	98.91%+/-0.01%(syst)+/-0.20%(stat)	1.56+/-0.24(stat)

Table 5: E10 cuts electrons efficiency and Background rejection after the tight cuts

In the end, totally we can get the total rejection power of cuts which is calculated by the number 3600 with the Tight cuts rejection power and the number 1.5 with the E_{10} cuts rejection power. After times them together, we can get the number $3600 \times 1.5 = 5400$. In A Toroidal LHC ApparatuS(ATLAS), the expected value for it is between 5000 to 10000, and in our case, we arrived the value for the expectation.

4 Milestone Achieved

- Submit my first journal paper: "Studies of granularity of a hadronic calorimeter for tens-of-TeV jets at a 100 TeV pp collider" to arxiv and the Journal of instrumentation(JINST), now is reviewed by the people in the journal.
- Submit my first conference paper: "Jet Substructure Variables with the SiFCC Detector at 100 TeV" to arxiv and is published by the Journal of Proceeding of Science(PoS).
- Accepted and report the poster with FCC detector studies in the International Conference of High Energy Physics in 2018(ICHEP2018).
- Accepted and report the two posters with HGCAL studies and FCC detector studies in the Taiwan Physics Society(TPS) annual meeting in 2019.

References